Systematic study of multi-quark states: A qq-qq-$\bar{q}$ configuration

Hongxia Huang,[1] Chengrong Deng,[1] Jialun Ping,[1] Fan Wang,[2] and T. Goldman[3]
[1]*Department of Physics, Nanjing Normal University, Nanjing 210097, People's Republic of China*
[2]*Department of Physics, Nanjing University, Nanjing 210093, People's Republic of China*
[3]*Theoretical Division, LANL, Los Alamos, New Mexico 87545, USA*
(Received 28 August 2007; published 7 February 2008)

A group theoretic method for the systematic study of multiquark states is developed. The calculation of matrix elements of many-body Hamiltonians is simplified by transforming the physical bases (quark cluster bases) to symmetry bases (group chain classified bases), where the fractional parentage expansion method can be used. A five-quark system is taken as the example in this study. The Jaffe–Wilczek qq-qq-$\bar{q}$ configuration is chosen as one of the examples to construct the physical bases and the transformation coefficients between physical bases and symmetry ones are shown to be related to the $SU_{mn} \supset SU_m \times SU_n$ isoscalar factors. A complete transformation coefficient table is obtained. The needed isoscalar factors and fractional parentage coefficients have been calculated with our new group representation theory and published before. Three quark models, the naive Glashow-Isgur model, the Salamanca chiral quark model, and quark delocalization color screening model, are used to show the general applicability of the new multiquark calculation method and general results of constituent quark models for five-quark states are given.

DOI: 10.1103/PhysRevC.77.025201 PACS number(s): 12.39.Mk, 12.39.Jh, 13.75.Jz, 24.85.+p

I. INTRODUCTION

Hadron (baryons and mesons) spectroscopy opens the gate for the development of the fundamental theory of the strong interaction: quantum chromodynamics (QCD). However, the nonperturbative complication of low energy QCD makes it impossible to calculate the hadron structure analytically from QCD directly. The unique color structure of the known hadrons makes the construction of quark models very efficient (Fig. 1). A variety of quark models that employ two-body interactions give a good description of hadron properties. (For baryon, three-body interactions can be well approximated by two-body interactions.) However, the unique color structure also limits our understanding of the properties of other color structures available in QCD. To understand low energy QCD, the study of systems with more quarks is indispensable. Hadron-hadron scattering provides a window on the nature of other color structures, but it is not enough because the colorless meson exchange model and chiral perturbation theory both describe the low energy hadron-hadron scattering data well. QCD does not rule out the existence of glueballs, quark-gluon hybrids, multiquark states, etc., based on the present understanding. Multiquark systems are important because they provide information on low energy QCD interaction, especially for complex color structures (Fig. 2).

Multiquark systems have been of interest since 1977, and although the interest fluctuates, it continues. The search for the H particle (six-quark system), which was predicted in 1977 by Jaffe [1] with the MIT bag model, has been unsuccessful for almost 30 years. In 1993, the dibaryon state d' appeared unexpectedly [2] (it was observed in double charge exchange reactions), but disappeared nine years later. Other six-quark states, d^* [3], $N\Omega$ [4], $\Omega\Omega$ [5], etc., had been proposed but none of them had been established experimentally. In 2003, the pentaquark state, Θ^+, aroused a new enthusiasm in multiquark systems. More than ten groups claimed that they observed the Θ^+ signal, but almost the same number of groups did not observe the signal [6,7]. Its appearance raised great trouble for the theory of hadron spectroscopy; almost none of the models constrained by hadron properties and hadron-hadron scattering can account for the Θ^+ [8,9]. In studying pentaquark Θ^+, various color and spatial structures of pentaquark have been proposed: color singlet hadron molecules $[K(q\bar{q})N(q^3)]$, color anti-triplet diquarks $[(qq)(qq)\bar{q}]$ [10], diquark-triquark $[qq$-$qq\bar{q}]$ [11], quark methane $[q^4\bar{q}]$ [12], etc. However, recent high statistic experiments have not confirmed the Θ^+ signal [13]. Today, about three years later, pentaquark Θ^+ seems to be about to disappear too.

After the pentaquark Θ^+ (a member of anti-decuplet), other states in 27-plet and 35-plet [14–16] were proposed. To understand the nucleon spin structure within the constituent quark model, the five-quark component is necessary [17]. Recently, to explain the strange magnetic moment of proton, the five-quark component was introduced in the nucleon [18].

Tetraquark states are of interest again both experimentally and theoretically because of new discoveries since 2003 [19].

Figure 2 shows possible color structures for five- and six-quark systems based on the lattice QCD calculation [20] and general color confinement idea. Clearly they have more possible color structures than two- and three-quark hadrons. Because of color confinement, only color singlet combinations of quarks can be separated. Colorful clusters are confined in a genuine multiquark system, which transits to color singlet subsystems through color flux rearrangement first and then decay. This induces a resonance similar to that of compound nucleus formation but due to color confinement and could be called color confinement resonance. To include these intermediate hidden color configurations in the quark model, a multichannel coupling calculation with multibody interactions is required. This is quite involved [21] and finding a method to make the calculation tractable is an important element in the study of multiquark systems with constituent quark models. Moreover up to now we have

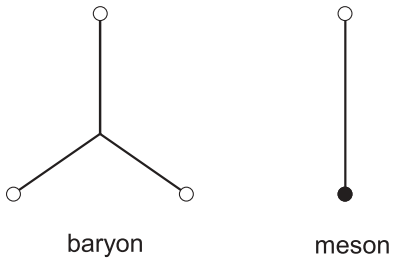

FIG. 1. The color structure of baryons and mesons.

had almost no idea about the transition interaction between different color configurations. The development of a model that includes the effects of these hidden color configurations is expected.

The group theory classification of four-, five-, and six-quark states has been published [16,22,23]. The fractional parentage (fp) expansion technique has been proven to be a powerful method for the study of the few-body problem. To fully employ the powerful group theoretic method for a quark model calculation one needs not only the fractional parentage expansion coefficients of the multiquark states but also a relation between various quark model states (hereafter called physical bases) and the group theoretical classification states (hereafter called symmetry bases). Such a method was developed and successfully applied in a systematic search of dibaryons [23–25]. The six-body Hamiltonian matrix elements on physical bases were calculated in the following procedure. First the physical bases were transformed to symmetry bases, then the calculation of six-body Hamiltonian matrix elements (with two-body interaction) on the symmetry bases, which could be reduced to four-body overlap and calculation of two-body matrix elements, was done by means of fractional parentage expansion. Last, the matrix elements on the symmetry bases were transformed back to physical bases.

The main content of this article is to provide the transformation coefficients between physical bases and symmetry bases of five-quark systems to facilitate the calculation of many-body Hamiltonian matrix elements. The physical bases discussed in this article are the Jaffe–Wilczek (JW) diquark

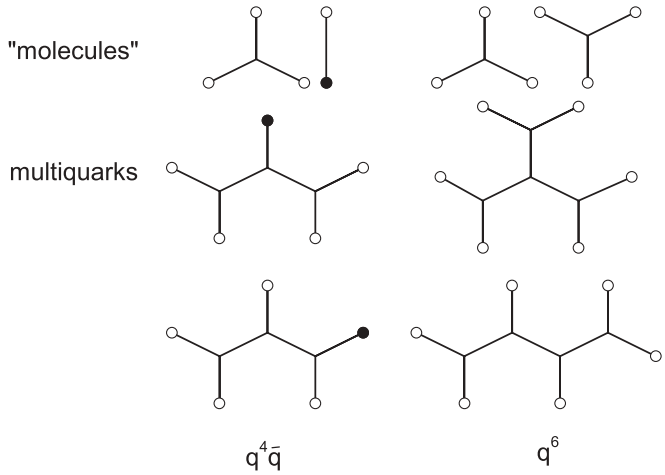

FIG. 2. The color structure of multiquark states.

model ones. Other useful physical bases are the meson-baryon bases, which will be given in another article. To illustrate the application of this group theory method for five-quark systems, three quark models are employed for pentaquark calculation. They are the naive quark model, i.e., the Glashow-Isgur model [26]; the Salamanca chiral quark model [27]; and the quark delocalization color screening model (QDCSM) developed by our group [28]. The calculation of the related fractional parentage coefficients are mentioned but the needed results have been published elsewhere [29,30].

In Sec. II, the physical bases and symmetry bases are introduced and the transformation between them is derived. The fractional parentage technique applied to calculate the matrix elements on the symmetry bases is also explained in this section. Section III explains the three quark models we used. The results of the systematic calculation of pentaquark in the u, d, s three-flavor world are given in Sec. IV. The last section gives the summary.

II. PHYSICAL BASES AND SYMMETRY BASES

The physical bases are constructed as follows, first the wave function of each quark cluster is constructed based on the group chain classification

$$\begin{array}{ccccccccccc} [1^n] & & [\nu] & & [\tilde{\nu}] & & [c] & & [\mu] & [f] & I \quad Y \quad J \\ \mathrm{SU}_{36} \supset & & \mathrm{SU}_2^x \times & \{ & \mathrm{SU}_{18} \supset & & \mathrm{SU}_3^c \times & [& \mathrm{SU}_6 \supset & (\ \mathrm{SU}_3^f \supset \mathrm{SU}_2^\tau \times \mathrm{U}_1^Y) \times & \mathrm{SU}_2^\sigma] \} \end{array}, \tag{1}$$

[the Young diagrams or quantum numbers for each group are also shown in Eq. (1)] then the quark cluster wave functions of the system are coupled to definite color, spin, and isospin quantum numbers by Clebsch-Gordan (CG) coefficients of color SU_3^c, spin SU_2^σ, and isospin SU_2^τ group and finally antisymmetrized.

For the Jaffe–Wilczek diquark configuration, the five quarks are separated into three clusters and form an isosceles triangle with the two strongly correlated pairs of quarks sitting at the bottom corners with separation S and the antiquark at the top with the height T (see Fig. 3). The diquark in the u, d, s three-flavor world is described by

$$\psi_2(q^2) = \left| \begin{array}{c} [\nu_2] W_{\nu_2} \\ [c_2]\, W_{c_2} [\mu_2][f_2] Y_2 I_2 M_{I_2} J_2 M_{J_2} \end{array} \right\rangle, \tag{2}$$

which is the basis vector belonging to the irreducible representations of group chain Eq. (1) with $n = 2$. $[\nu]$, W, etc., are the Young diagrams, Weyl tableaux, etc., describing the permutation and SU_n symmetries. In our calculation,

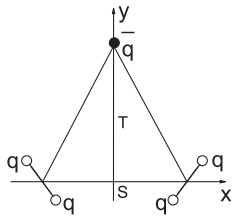

FIG. 3. The Jaffe–Wilczek configuration of pentaquark.

the ground state diquarks are assumed to be in the totally symmetric orbital state $[\nu_2] = [2]$. The cluster basis for the four-quark system can be defined as

$$\Psi_{\alpha_4 k_4}(q^4) = \mathcal{A}\,[\psi_2(q_1q_2)\psi_2(q_3q_4)]^{[c_4]I_4J_4}_{W_{c_4}M_{I_4}M_{J_4}}, \tag{3}$$

where $\mathcal{A}$ is a normalized antisymmetric operator for the four-quark system and [ ] means coupling in terms of the SU_3^c, SU_2^τ, SU_2^σ CG coefficients so that it has color symmetry $[c_4]W_{c_4}$, isospin $I_4M_{I_4}$, and spin $J_4M_{J_4}$. $\alpha_4 = (Y_4I_4J_4), k_4$ represents the quantum numbers $\nu_2, \nu_2', c_2, \ldots, J_2'$. The cluster basis for the five-quark system can be obtained by coupling the antiquark basis to the four-quark basis in terms of the SU_3^c, SU_2^τ, SU_2^σ CG coefficients,

$$\Psi_{\alpha k}(q^4\bar{q}) = \left[\Psi_{\alpha_4 k_4}(q^4))\psi_{[\bar{c}]\bar{I}\bar{J}}(\bar{q}_5)\right]^{[c]IJ}_{WM_IM_J}. \tag{4}$$

The symmetry basis of the four-quark system is just the group chain [Eq. (1)] classification basis ($n = 4$),

$$\Phi_{\alpha_4 K_4}(q^4) = \left| \begin{matrix} [\nu_4]W_{\nu_4} \\ [c_4]\,W_{c_4}[\mu_4][f_4]Y_4I_4M_{I_4}J_4M_{J_4} \end{matrix} \right\rangle, \tag{5}$$

where K_4 stands for $\nu_4\mu_4 f_4$. Similar to Eq. (4), the symmetry basis for the five-quark system is

$$\Phi_{\alpha K}(q^4\bar{q}) = \left[\Phi_{\alpha_4 K_4}(q^4))\psi_{[\bar{c}]\bar{I}\bar{J}}(\bar{q}_5)\right]^{[c]IJ}_{WM_IM_J}. \tag{6}$$

The cluster bases and symmetry bases for the five-quark system can be transformed to each other [23,24,31,32].

$$\begin{aligned}\Psi_{\alpha k}(q^4\bar{q}) &= \sum_K C_{kK}\Phi_{\alpha K}(q^4\bar{q}) \\ &= \sum_{\tilde{\nu}_4\mu_4 f_4} C^{[\tilde{\nu}_4][c_4][\mu_4]}_{[\tilde{\nu}_2][c_2][\mu_2],[\tilde{\nu}_2'][c_2'][\mu_2']} C^{[\mu_4][f_4][J_4]}_{[\mu_2][f_2][J_2],[\mu_2'][f_2'][J_2']} \\ &\quad \times C^{[f_4]Y_4I_4}_{[f_2]Y_2I_2,[f_2']Y_2'I_2'}\Phi_{\alpha K}(q^4\bar{q}),\end{aligned} \tag{7}$$

C's are the isoscalar factors of $SU_{mn} \supset SU_m \times SU_n$, which can be obtained from the book [30].

A physical five-quark state with quantum number $\alpha = (Y\,I\,J)$ is expressed as a channel coupling wave function,

$$\Psi_\alpha(q^4\bar{q}) = \sum_k C_k\Psi_{\alpha k}(q^4\bar{q}). \tag{8}$$

The channel coupling coefficient C_k is determined by the diagonalization of the five-quark Hamiltonian as usual. The calculation of Hamiltonian matrix elements in the cluster bases is tedious and it can be replaced by the matrix elements in the symmetry bases by the transformation Eq. (7),

$$\langle\Psi_{\alpha k}|H|\Psi_{\alpha k'}\rangle = \sum_{K,K'} C_{kK}C_{k'K'}\,\langle\Phi_{\alpha K}|\,H\,|\Phi_{\alpha K'}\rangle\,. \tag{9}$$

In the symmetry bases, the matrix elements $\langle\Phi_{\alpha K}|H|\Phi_{\alpha K'}\rangle$ can be calculated by the well-known fp expansion method. Because there is an antiquark, we have to use different fp expansions for qq interaction and $q\bar{q}$ interaction. For qq interaction, $4 \to 2+2$ is used.

$$\begin{aligned}\langle\Phi_{\alpha K}\,|H_{34}|\,\Phi_{\alpha K'}\rangle = \sum_{1,2} & C^{[1^4][\nu_4][\tilde{\nu}_4]}_{[1^2][\nu_1][\tilde{\nu}_1],[1^2][\nu_2][\tilde{\nu}_2]} C^{[\tilde{\nu}_4][c_4][\mu_4]}_{[\tilde{\nu}_1][c_1][\mu_1],[\tilde{\nu}_2][c_2][\mu_2]} C^{[\mu_4][f_4]J_4}_{[\mu_1][f_1]J_1,[\mu_2][f_2]J_2} C^{[f_4]Y_4I_4}_{[f_1]Y_1I_1,[f_2]Y_2I_2} \\ & \times C^{[1^4][\nu_4][\tilde{\nu}_4]}_{[1^2][\nu_1'][\tilde{\nu}_1'],[1^2][\nu_2'][\tilde{\nu}_2']} C^{[\tilde{\nu}_4][c_4][\mu_4]}_{[\tilde{\nu}_1'][c_1'][\mu_1'],[\tilde{\nu}_2'][c_2'][\mu_2']} C^{[\mu_4][f_4]J_4}_{[\mu_1'][f_1']J_1',[\mu_2'][f_2']J_2'} C^{[f_4]Y_4I_4}_{[f_1']Y_1'I_1',[f_2']Y_2'I_2'} \\ & \times C^{[\nu_4]W_{x_4}}_{[\nu_1]W_{x_1},[\nu_2]W_{x_2}} C^{[\nu_4]W_{x_4'}}_{[\nu_1']W_{x_1'},[\nu_2']W_{x_2'}} \langle\alpha_1K_1|\alpha_1'K_1'\rangle\langle\alpha_2K_2|H_{34}|\alpha_2'K_2'\rangle.\end{aligned} \tag{10}$$

Here C's are the $SU_{mn} \supset SU_m \times SU_n$ isoscalar factors, $\langle\alpha_1K_1|\alpha_1'K_1'\rangle$ is the two-quark overlap, $\langle\alpha_2K_2|H_{34}|\alpha_2'K_2'\rangle$ is the two-body matrix element, and H_{34} represents the two-body operator for the second pair. The interacting pair number is $C_2^4 = 6$. For $q\bar{q}$ interaction, $4 \to 3+1$ is used.

$$\begin{aligned}\langle\Phi_{\alpha K}\,|H_{45}|\,\Phi_{\alpha K'}\rangle = \sum_{3,1} & C^{[1^4][\nu_4][\tilde{\nu}_4]}_{[1^3][\nu_3][\tilde{\nu}_3],[1][\nu_1][\tilde{\nu}_1]} C^{[\tilde{\nu}_4][c_4][\mu_4]}_{[\tilde{\nu}_3][c_3][\mu_3],[\tilde{\nu}_1][c_1][\mu_1]} C^{[\mu_4][f_4]J_4}_{[\mu_3][f_3]J_3,[\mu_1][f_1]J_1} C^{[f_4]Y_4I_4}_{[f_3]Y_3I_3,[f_1]Y_1I_1} \\ & \times C^{[1^4][\nu_4][\tilde{\nu}_4]}_{[1^3][\nu_3'][\tilde{\nu}_3'],[1][\nu_1'][\tilde{\nu}_1']} C^{[\tilde{\nu}_4][c_4][\mu_4]}_{[\tilde{\nu}_3'][c_3'][\mu_3'],[\tilde{\nu}_1'][c_1'][\mu_1']} C^{[\mu_4][f_4]J_4}_{[\mu_3'][f_3']J_3',[\mu_1'][f_1']J_1'} C^{[f_4]Y_4I_4}_{[f_3']Y_3'I_3',[f_1']Y_1'I_1'} \\ & \times U(c_3c_1cc_{\bar{1}};c_4c_2)U(I_3I_1I\,I_{\bar{1}};I_4I_2)U(J_3J_1J\,J_{\bar{1}};J_4J_2)\end{aligned}$$

$$\times U(c_3' c_1' c c_1'; c_4 c_2') U(I_3' I_1' I I_1'; I_4 I_2') U(J_3' J_1' J J_1'; J_4 J_2')$$
$$\times C^{[\nu_4]W_{x_4}}_{[\nu_3]W_{x_3},[\nu_1]W_{x_1}} C^{[\nu_4]W_{x_4'}}_{[\nu_3']W_{x_3'},[\nu_1']W_{x_1'}} \langle \alpha_3 K_3 | \alpha_3' K_3' \rangle \langle \alpha_2 K_2 | H_{45} | \alpha_2' K_2' \rangle. \quad (11)$$

Here U's are Racah coefficients, $\langle \alpha_3 K_3 | \alpha_3' K_3' \rangle$ is the three-quark overlap, $\langle \alpha_2 K_2 | H_{45} | \alpha_2' K_2' \rangle$ is the two-body matrix element, and H_{45} represents the quark-antiquark operator. The interacting pair number is $C_1^4 = 4$. The calculation of every factor in the above equations can be found in Ref. [24]. Last, the matrix elements of the five-body Hamiltonian can be obtained,

$$\langle \Phi_{\alpha K} | H_5 | \Phi_{\alpha K'} \rangle = 6 \langle \Phi_{\alpha K} | H_{34} | \Phi_{\alpha K'} \rangle + 4 \langle \Phi_{\alpha K} | H_{45} | \Phi_{\alpha K'} \rangle. \quad (12)$$

The matrix elements of the five-body Hamiltonian on the physical bases can be obtained from the matrix elements on the symmetry bases and the transformation coefficients.

III. QUARK MODELS AND CALCULATION METHOD

A. Naive quark cluster model

The Hamiltonian of the naive quark cluster model is [26]

$$H = \sum \left(m_i + \frac{p_i^2}{2m_i} \right) - T_{\rm CM} + \sum_{i>j=1}^{5} \left(V_{ij}^C + V_{ij}^G \right), \quad (13)$$

$$T_{\rm CM} = \frac{1}{2M} \left(\sum_{i=1}^{5} \vec{p}_i \right)^2, \quad M = \sum_{i=1}^{5} m_i, \quad (14)$$

$$V_{ij}^G = \alpha_s \frac{\vec{\lambda}_i \cdot \vec{\lambda}_j}{4} \left[\frac{1}{r_{ij}} - \frac{\pi \delta(\vec{r})}{2} \left(\frac{1}{m_i^2} + \frac{1}{m_j^2} + \frac{4 \vec{\sigma}_i \cdot \vec{\sigma}_j}{3 m_i m_j} \right) \right], \quad (15)$$

$$V_{ij}^C = -\alpha_c \vec{\lambda}_i \cdot \vec{\lambda}_j r_{ij}^2. \quad (16)$$

All of the symbols retain their original meaning as described in Ref. [26].

The single particle orbital wave function in the naive quark model is as follows:

$$\phi_L(\vec{r}) \equiv |L\rangle = \left(\frac{1}{\pi b^2} \right)^{\frac{3}{4}} e^{-\frac{1}{2b^2}(\vec{r} + \frac{\vec{s}}{2})^2}, \quad (17)$$

$$\phi_R(\vec{r}) \equiv |R\rangle = \left(\frac{1}{\pi b^2} \right)^{\frac{3}{4}} e^{-\frac{1}{2b^2}(\vec{r} - \frac{\vec{s}}{2})^2}, \quad (18)$$

$$\phi_U(\vec{r}) \equiv |U\rangle = \left(\frac{1}{\pi b^2} \right)^{\frac{3}{4}} e^{-\frac{1}{2b^2}(\vec{r} - \vec{T})^2}, \quad (19)$$

where $\frac{\vec{s}}{2}$ and $\vec{T}$ are the coordinates of the reference center of each quark cluster.

B. Chiral quark model

We choose the Salamanca model as representative of this class of models. Details of the model can be found in Ref. [27].

Here we display only the Hamiltonian,

$$H = \sum \left(m_i + \frac{p_i^2}{2m_i} \right) - T_{\rm CM} + \sum_{i>j=1}^{5} \left(V_{ij}^C + V_{ij}^G + V_{ij}^\chi + V_{ij}^\sigma \right), \quad (20)$$

$$V_{ij}^\chi = \frac{1}{3} \alpha_{\rm ch} \frac{\Lambda^2}{\Lambda^2 - m_\chi^2} m_\chi \left[\frac{e^{-m_\chi r_{ij}}}{m_\chi r_{ij}} - \frac{\Lambda^3}{m_\pi^3} \frac{e^{-m_\Lambda r_{ij}}}{m_\Lambda r_{ij}} \right] \vec{\sigma}_i \cdot \vec{\sigma}_j \vec{\lambda}_i \cdot \vec{\lambda}_j, \quad \chi = \pi, K, \eta \quad (21)$$

$$V_{ij}^\sigma = -\alpha_{\rm ch} \frac{4 m_q^2}{m_\pi^2} \frac{\Lambda^2}{\Lambda^2 - m_\sigma^2} m_\sigma \left[\frac{e^{-m_\sigma r_{ij}}}{m_\sigma r_{ij}} - \frac{\Lambda}{m_\sigma} \frac{e^{-\Lambda r_{ij}}}{m_\Lambda r_{ij}}) \right],$$

V_{ij}^χ and V_{ij}^σ are pseudoscalar and scalar meson exchange potentials. The color confinement and one-gluon-exchange potentials and the single particle orbital wave functions are the same as those in the naive quark model.

C. Quark delocalization, color screening model

The quark delocalization, color screening model (QDCSM) is an extension of the naive quark cluster model and was developed with the aim of addressing multiquark systems [28,33]. First, a quark delocalization similar to the percolation of electrons in atoms is introduced to take into account the contribution of orbital excitation or the mutual distortion of hadrons in the interaction region. Second, a different parametrization of the confinement interaction is assumed for the quark pairs in different states. The parametrization is an effort to account for the QCD interactions corresponding to various hidden color configurations in the multiquark system that have not been modeled in the two-body interaction model. The main advantage of QDCSM is that it allows the multiquark system to choose its most favorable configuration through its own dynamics. This is accomplished by varying the energy of the system with respect to the delocalization parameter, which is a tentative approach to take into account the self-consistency of the quark and gluon distributions in the course of the hadron interaction process.

This model reproduces the existing baryon-baryon interaction data well [28,33] (bound-state deuteron as well as NN, $N\Lambda$, and $N\Sigma$ scattering). It is therefore interesting to apply the QDCSM to study the pentaquark system. Some generalizations are needed here: the quark can delocalize among clusters and the color confinement between quarks in different clusters is screened as before, but now the clusters may be colorful as well as colorless. We admit there should be a difference in the QCD vacuum between colorless hadrons and colorful ones and so color screening should be different but, to avoid new parameters, we employ the original one tentatively.

The quark delocalization is realized by replacing the single particle orbital wave functions (ϕ_L and ϕ_R by ψ_l and ψ_r):

$$\begin{aligned}
\psi_l &= (\phi_L + \epsilon_1\phi_R + \epsilon_2\phi_U)/N_l, \\
\psi_r &= (\phi_R + \epsilon_1\phi_L + \epsilon_2\phi_U)/N_r, \\
\psi_u &= (\phi_U + \epsilon_3\phi_L + \epsilon_3\phi_R)/N_u,
\end{aligned} \tag{22}$$

$$\begin{aligned}
N_l &= \sqrt{1+\epsilon_1^2+\epsilon_2^2+2\epsilon_1\langle L|R\rangle+2\epsilon_2\langle L|U\rangle+2\epsilon_1\epsilon_2\langle R|U\rangle}, \\
N_r &= \sqrt{1+\epsilon_1^2+\epsilon_2^2+2\epsilon_1\langle L|R\rangle+2\epsilon_2\langle R|U\rangle+2\epsilon_1\epsilon_2\langle L|U\rangle}, \\
N_u &= \sqrt{1+2\epsilon_3^2+2\epsilon_3\langle U|L\rangle+2\epsilon_3\langle U|R\rangle+2\epsilon_3^2\langle L|R\rangle},
\end{aligned} \tag{23}$$

here, ϵ_1, ϵ_2, and ϵ_3 are variational parameters determined by the dynamics of the multiquark system rather than adjustable (fitting) parameters.

The color screeening is realized by reparametrizing the color confinement interaction as follows:

$$V_{ij}^C = \begin{cases} -\alpha_c \vec{\lambda}_i \cdot \vec{\lambda}_j r_{ij}^2 & \text{if } i,j \text{ occur in orbits with the same reference center} \\ -\alpha_c \vec{\lambda}_i \cdot \vec{\lambda}_j \frac{1-e^{-\mu r_{ij}^2}}{\mu} & \text{if } i,j \text{ occur in orbits with different reference centers.} \end{cases} \tag{24}$$

Details of the model can be found in Ref. [33].

The adiabatic approximation is used here to do a systematic study. For each given separation S and T, the energy of the five-quark state is calculated. (For QDCSM, the energy for given S and T is obtained by varying the energy with the delocalization parameters.) If minimum energy at finite separations S_0 and T_0 exists, then the energy $E(S_0, T_0)$ is taken as the mass of the state.

IV. RESULTS AND DISCUSSIONS

The index of diquark clusters is given in Table I. The calculated transformation coefficients are listed in Table II. (To save space, only several examples of the transformation coefficients are listed here. The complete table of transformation coefficients can be found in Ref. [34].) In this table, all the channels are included, so it can be used to expand the physical bases in terms of the symmetry bases, and vice versa. This table can be used for any quark model Hamiltonian but is restricted to JW qq-qq-$\bar{q}$ cluster configuration. For meson-baryon cluster configuration one needs other transformation coefficients that will be given in a forthcoming article.

TABLE I. Index of diquark clusters.

	$[\nu_2]$	$[c_2]$	$[f_2]$	$[\sigma_2]$	Y_2	I_2
1	[2]	[2]	[2]	[11]	2/3	1
2	[2]	[2]	[2]	[11]	−1/3	1/2
3	[2]	[2]	[2]	[11]	−4/3	0
4	[2]	[2]	[11]	[2]	2/3	0
5	[2]	[2]	[11]	[2]	−1/3	1/2
6	[2]	[11]	[2]	[2]	2/3	1
7	[2]	[11]	[2]	[2]	−1/3	1/2
8	[2]	[11]	[2]	[2]	−4/3	0
9	[2]	[11]	[11]	[11]	2/3	0
10	[2]	[11]	[11]	[11]	−1/3	1/2

All possible states within the u, d, s three-flavor world have been calculated. Both single channel and channel coupling calculations have been carried out with three quark models: the naive quark model, the chiral quark model, and the QDCSM. The results are listed in Table III. Because the parity is a good quantum number, the results for positive and negative parity states are listed separately. To save space, only the lowest single channel (sc) and channel coupling (cc) results are given. All the states with $Y = 2$ are given, and several states with $Y \neq 2$ are given, because most states with $Y \neq 2$ have quite similar features to the ones with $Y = 2$. Some general features are listed below.

(i) The parity of the lowest channel is negative in all three quark models, which is different from Jaffe–Wilczek's estimation. The diquark with orbital, color, spin, flavor symmetry, [2], [11], [11], [11], does have the lowest energy under the color-magnetic interaction; however, the Pauli principle excludes the S-wave orbital motion between two such diquarks. The P-wave excitation and the "residue" interaction between two diquarks make the energy of the JW state higher than that of the state where two diquarks have the symmetry [2] × [2] (orbital), [11] × [2] (color), [11] × [2] (spin), and [11] × [11] (flavor), where the S-wave orbital is permitted.

(ii) Generally there exist effective attractions for both positive and negative parity states; thus forming resonance in both parity states is possible. This is due to the hidden color structure of the JW configuration as discussed in the Introduction. However in most cases, the attraction is not enough to make the energy lower than the corresponding threshold, i.e., the sum of corresponding baryon and meson masses. Therefore, there will be no narrow resonances but there is a special mechanism to prevent the decay. Figure 4 gives the effective potential

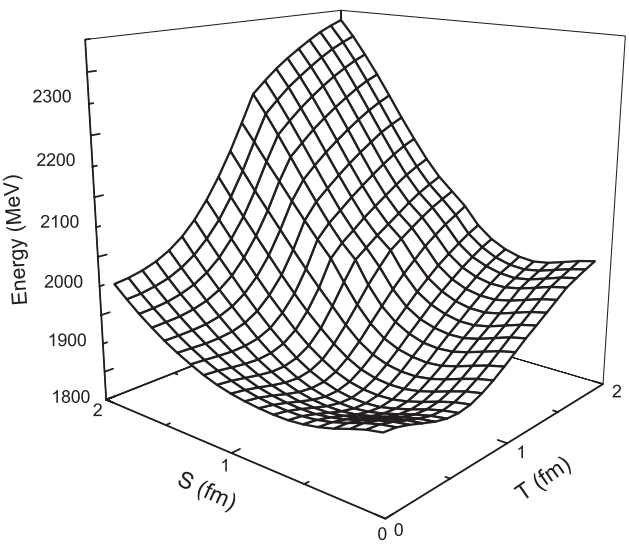

FIG. 4. The effective potential for $YIJ = 20\frac{1}{2}$ with channel coupling in QDCSM.

TABLE II. Transformation coefficients between physical bases and symmetry bases. The column labels are $[\nu_4]$, $[\mu_4]$, $[f_4]$, $[J_4]$, I_4. For the first four labels, 1 stands for the symmetry label [4]; 2, [31]; 3, [22]; 4, [211], and for the last one, 1 stands for $I = 2$; 2, $\frac{3}{2}$; 3, 1; 4, $\frac{1}{2}$; 5, 0. The row label $D_1 D_2$ stands for two diquark clusters, the index of which is listed in Table I. $[J_4]$, I_4 are the same labels as the one in column labels.

				$Y=2$	$I=0$	$J=\frac{1}{2}$	$Y_4=\frac{4}{3}$			
D_1	D_2	J_4	I_4	12325	22325	24325	32325	34325	21335	23335
1	6	2	5	$-\frac{1}{6}$	0	0	$-\frac{1}{12}$	$-\frac{3}{4}$	0	0
4	9	2	5	$\frac{1}{2}$	0	0	$\frac{1}{4}$	$-\frac{1}{4}$	0	0
6	1	2	5	0	$\frac{1}{4}$	$-\frac{3}{4}$	0	0	0	0
6	6	2	5	$-\frac{1}{3}$	0	0	$\frac{2}{3}$	0	0	0
6	6	3	5	0	0	0	0	0	$\frac{1}{2}$	$-\frac{1}{2}$
9	4	2	5	0	$-\frac{3}{4}$	$-\frac{1}{4}$	0	0	0	0
9	9	3	5	0	0	0	0	0	$\frac{1}{2}$	$\frac{1}{2}$

				$Y=1$	$I=\frac{3}{2}$	$J=\frac{1}{2}$	$Y_4=\frac{1}{3}$									
D_1	D_2	J_4	I_4	12122	12222	22122	22222	24222	32122	32222	34222	12232	22232	24232	32232	34232	21222	23222	23132
1	7	2	2	$\frac{1}{3}$	$-\frac{1}{6}$	0	0	0	$\frac{1}{6}$	$-\frac{1}{12}$	$-\frac{1}{4}$	0	0	0	0	0	0	0	0
1	10	3	2	0	0	0	0	0	0	0	0	$\frac{1}{2}$	0	0	$\frac{1}{4}$	$-\frac{1}{4}$	0	0	0
2	6	2	2	$\frac{1}{3}$	$\frac{1}{6}$	0	0	0	$\frac{1}{6}$	$\frac{1}{12}$	$\frac{1}{4}$	0	0	0	0	0	0	0	0
5	6	2	2	0	0	0	$\frac{1}{2}$	$\frac{1}{2}$	0	0	0	0	0	0	0	0	0	0	0
5	6	3	2	0	0	0	0	0	0	0	0	$-\frac{1}{6}$	0	0	$-\frac{1}{12}$	$-\frac{3}{4}$	0	0	0
6	2	2	2	0	0	$-\frac{1}{2}$	$-\frac{1}{4}$	$\frac{1}{4}$	0	0	0	0	0	0	0	0	0	0	0
6	5	2	2	0	$-\frac{1}{3}$	0	0	0	0	$-\frac{1}{6}$	$\frac{1}{2}$	0	0	0	0	0	0	0	0
6	5	3	2	0	0	0	0	0	0	0	0	0	$\frac{1}{4}$	$-\frac{3}{4}$	0	0	0	0	0
6	7	2	2	$-\frac{1}{3}$	0	0	0	0	$\frac{2}{3}$	0	0	0	0	0	0	0	0	0	0
6	7	3	2	0	0	0	0	0	0	0	0	0	0	0	0	0	0	0	−1
6	10	2	2	0	0	0	0	0	0	0	0	0	0	0	0	0	$\frac{2}{3}$	$\frac{1}{3}$	0
7	1	2	2	0	0	$-\frac{1}{2}$	$\frac{1}{4}$	$-\frac{1}{4}$	0	0	0	0	0	0	0	0	0	0	0
7	6	2	2	0	0	0	0	0	0	0	0	0	0	0	0	0	$\frac{1}{3}$	$-\frac{2}{3}$	0
7	6	3	2	0	0	0	0	0	0	0	0	$-\frac{1}{3}$	0	0	$\frac{2}{3}$	0	0	0	0
10	1	3	2	0	0	0	0	0	0	0	0	0	$-\frac{3}{4}$	$-\frac{1}{4}$	0	0	0	0	0
10	6	2	2	0	$-\frac{1}{3}$	0	0	0	0	$\frac{2}{3}$	0	0	0	0	0	0	0	0	0

				$Y=0$	$I=2$	$J=\frac{1}{2}$	$Y_4=\frac{1}{3}$									
D_1	D_2	J_4	I_4	12122	12222	22122	22222	24222	32122	32222	34222	12232	22232	24232	32232	34232	21222	23222	23132
1	7	2	2	$\frac{1}{3}$	$-\frac{1}{6}$	0	0	0	$\frac{1}{6}$	$-\frac{1}{12}$	$-\frac{1}{4}$	0	0	0	0	0	0	0	0
1	10	3	2	0	0	0	0	0	0	0	0	$\frac{1}{2}$	0	0	$\frac{1}{4}$	$-\frac{1}{4}$	0	0	0
2	6	2	2	$\frac{1}{3}$	$\frac{1}{6}$	0	0	0	$\frac{1}{6}$	$\frac{1}{12}$	$\frac{1}{4}$	0	0	0	0	0	0	0	0
5	6	2	2	0	0	0	$\frac{1}{2}$	$\frac{1}{2}$	0	0	0	0	0	0	0	0	0	0	0
5	6	3	2	0	0	0	0	0	0	0	0	$-\frac{1}{6}$	0	0	$-\frac{1}{12}$	$-\frac{3}{4}$	0	0	0
6	2	2	2	0	0	$-\frac{1}{2}$	$-\frac{1}{4}$	$\frac{1}{4}$	0	0	0	0	0	0	0	0	0	0	0
6	5	2	2	0	$-\frac{1}{3}$	0	0	0	0	$-\frac{1}{6}$	$\frac{1}{2}$	0	0	0	0	0	0	0	0
6	5	3	2	0	0	0	0	0	0	0	0	0	$\frac{1}{4}$	$-\frac{3}{4}$	0	0	0	0	0
6	7	2	2	$-\frac{1}{3}$	0	0	0	0	$\frac{2}{3}$	0	0	0	0	0	0	0	0	0	0
6	7	3	2	0	0	0	0	0	0	0	0	0	0	0	0	0	0	0	−1
6	10	2	2	0	0	0	0	0	0	0	0	0	0	0	0	0	$\frac{2}{3}$	$\frac{1}{3}$	0
7	1	2	2	0	0	$-\frac{1}{2}$	$\frac{1}{4}$	$-\frac{1}{4}$	0	0	0	0	0	0	0	0	0	0	0
7	6	2	2	0	0	0	0	0	0	0	0	0	0	0	0	0	$\frac{1}{3}$	$-\frac{2}{3}$	0
7	6	3	2	0	0	0	0	0	0	0	0	$-\frac{1}{3}$	0	0	$\frac{2}{3}$	0	0	0	0
10	1	3	2	0	0	0	0	0	0	0	0	0	$-\frac{3}{4}$	$-\frac{1}{4}$	0	0	0	0	0
10	6	2	2	0	$-\frac{1}{3}$	0	0	0	0	$\frac{2}{3}$	0	0	0	0	0	0	0	0	0

for the channel coupling result of Θ^+ in QDCSM. The other two models have effective potentials similar to those of QDCSM. Other states have effective potentials similar to that of Θ^+ shown in Fig. 4. In QDCSM, the mass of Θ^+ is 1786 MeV, which is too high to match the experimentally claimed 1540 MeV. The other two models give even higher masses of Θ^+. For Ξ^{--}, the QDCSM mass is about 1884 MeV, a little higher than the claimed 1862 MeV. The other two models' masses of Ξ^{--} are much higher (1974 MeV for the chiral quark model and 2145 MeV for the naive quark model).

(iii) The spectroscopy of QDCSM and the spectroscopy of the chiral quark model are quite similar except for a mass shift. This result is quite consistent with our former work on *NN* interaction [35], where the two models with quite different mechanisms of intermediate range attraction give similar results of deuteron properties and *NN* scattering phase shifts and show the σ meson

TABLE III. Mass of the pentaquark in various quark models (S, T in fm and E in MeV).

Y	I	J^P		QDCSM						Chiral quark model			Naive quark model		
				E	S	T	ϵ_1	ϵ_2	ϵ_3	E	S	T	E	S	T
2	2	$\frac{5}{2}^+$	sc	2150	1.4	0.6	0.8	0.99	0.8	2387	0.7	0.1	2498	0.7	0.1
2	2	$\frac{3}{2}^+$	sc	2113	1.3	0.6	0.9	0.99	0.99	2338	0.6	0.1	2463	0.7	0.1
			cc	2107	1.3	0.6	0.9	0.99	0.99	2330	0.6	0.1	2453	0.7	0.1
2	2	$\frac{3}{2}^-$	sc	2040	1.0	0.9	0.4	0.7	0.99	2266	0.5	0.1	2342	0.5	0.1
			cc	2038	1.0	0.9	0.2	0.6	0.99	2244	0.6	0.1	2316	0.6	0.1
2	2	$\frac{1}{2}^+$	sc	2255	1.2	0.8	0.1	0.5	0.9	2495	0.8	0.1	2569	0.8	0.1
			cc	2246	1.2	0.7	0.1	0.6	0.8	2484	0.8	0.1	2556	0.7	0.1
2	2	$\frac{1}{2}^-$	sc	2082	1.0	0.9	0.4	0.7	0.99	2329	0.6	0.1	2416	0.6	0.1
			cc	2080	1.0	0.9	0.1	0.5	0.99	2311	0.7	0.1	2393	0.7	0.1
2	1	$\frac{5}{2}^+$	sc	2245	1.1	0.8	0.9	0.99	0.9	2519	0.5	0.1	2608	0.5	0.1
2	1	$\frac{5}{2}^-$	sc	2011	1.0	0.8	0.5	0.8	0.99	2223	0.4	0.1	2321	0.4	0.1
			cc	2009	1.0	0.8	0.2	0.6	0.99	2206	0.6	0.1	2298	0.6	0.1
2	1	$\frac{3}{2}^+$	sc	2037	1.2	0.6	0.3	0.6	0.9	2209	0.6	0.1	2405	0.7	0.1
			cc	1977	1.3	0.3	0.7	0.99	0.6	2148	0.5	0.1	2377	0.6	0.1
2	1	$\frac{3}{2}^-$	sc	1909	0.9	0.8	0.3	0.6	0.99	2061	0.4	0.1	2228	0.4	0.1
			cc	1882	0.8	0.8	0.1	0.5	0.99	2014	0.5	0.1	2157	0.5	0.1
2	1	$\frac{1}{2}^+$	sc	2010	1.2	0.5	0.3	0.6	0.9	2172	0.6	0.1	2377	0.7	0.1
			cc	1931	1.2	0.3	0.8	0.99	0.8	2089	0.4	0.1	2331	0.6	0.1
2	1	$\frac{1}{2}^-$	sc	1886	0.9	0.8	0.6	0.8	0.99	2034	0.3	0.1	2231	0.4	0.1
			cc	1868	0.8	0.8	0.1	0.5	0.99	2000	0.4	0.1	2181	0.5	0.1
2	0	$\frac{5}{2}^+$	sc	2242	1.2	0.7	0.1	0.6	0.8	2483	0.7	0.1	2557	0.7	0.1
2	0	$\frac{3}{2}^+$	sc	2117	1.0	0.7	0.9	0.8	0.99	2326	0.4	0.1	2488	0.7	0.1
			cc	2079	1.1	0.6	0.8	0.99	0.9	2273	0.3	0.1	2451	0.5	0.1
2	0	$\frac{3}{2}^-$	sc	1871	0.8	0.8	0.3	0.6	0.99	2011	0.3	0.1	2219	0.4	0.1
			cc	1870	0.8	0.8	0.3	0.6	0.99	2007	0.4	0.1	2207	0.5	0.1
2	0	$\frac{1}{2}^+$	sc	1915	1.1	0.5	0.1	0.4	0.9	2054	0.7	0.1	2316	0.7	0.1
			cc	1868	1.2	0.1	0.5	0.99	0.5	1999	0.5	0.1	2280	0.6	0.1
2	0	$\frac{1}{2}^-$	sc	1787	0.8	0.7	0.3	0.6	0.99	1887	0.3	0.1	2109	0.3	0.1
			cc	1786	0.8	0.7	0.1	0.5	0.99	1886	0.3	0.1	2100	0.5	0.1
1	$\frac{5}{2}$	$\frac{5}{2}^+$	sc	2103	1.4	0.6	0.9	0.99	0.7	2366	0.7	0.1	2457	0.7	0.1
1	$\frac{3}{2}$	$\frac{5}{2}^+$	sc	2041	1.4	0.5	0.7	0.99	0.6	2273	0.6	0.1	2457	0.7	0.1
			cc	2040	1.4	0.5	0.7	0.99	0.6	2271	0.6	0.1	2457	0.7	0.1
1	$\frac{1}{2}$	$\frac{5}{2}^+$	sc	2150	1.2	0.7	0.8	0.99	0.9	2424	0.5	0.1	2531	0.8	0.1
			cc	2149	1.2	0.7	0.7	0.99	0.8	2421	0.5	0.1	2531	0.8	0.1
1	$\frac{1}{2}$	$\frac{5}{2}^-$	sc	1906	1.0	0.8	0.5	0.8	0.99	2123	0.4	0.1	2289	0.4	0.1
			cc	1903	1.0	0.8	0.2	0.6	0.99	2101	0.6	0.1	2260	0.6	0.1
0	2	$\frac{5}{2}^+$	sc	2161	1.4	0.6	0.8	0.99	0.7	2400	0.7	0.1	2483	0.7	0.1
			cc	2161	1.4	0.6	0.8	0.99	0.7	2400	0.7	0.1	2483	0.7	0.1
0	2	$\frac{5}{2}^-$	sc	2002	1.0	0.8	0.5	0.8	0.99	2211	0.4	0.1	2319	0.4	0.1
			cc	2001	1.0	0.8	0.2	0.6	0.99	2196	0.6	0.1	2296	0.6	0.1
0	1	$\frac{5}{2}^+$	sc	2110	1.4	0.5	0.7	0.99	0.6	2323	0.6	0.1	2483	0.7	0.1
			cc	2109	1.4	0.5	0.7	0.99	0.6	2319	0.6	0.1	2483	0.7	0.1
0	1	$\frac{5}{2}^-$	sc	1944	0.9	0.8	0.5	0.7	0.99	2120	0.4	0.1	2319	0.4	0.1
			cc	1941	0.9	0.8	0.2	0.6	0.99	2106	0.5	0.1	2296	0.6	0.1
0	0	$\frac{5}{2}^+$	sc	2215	1.2	0.7	0.1	0.6	0.8	2444	0.7	0.1	2564	0.7	0.1
			cc	2211	1.2	0.7	0.2	0.7	0.8	2440	0.7	0.1	2563	0.7	0.1
0	0	$\frac{5}{2}^-$	sc	1985	1.0	0.8	0.5	0.8	0.99	2181	0.4	0.1	2321	0.4	0.1
			cc	1983	0.9	0.8	0.2	0.6	0.99	2164	0.5	0.1	2301	0.6	0.1
-1	$\frac{3}{2}$	$\frac{1}{2}^+$	sc	2109	1.1	0.5	0.1	0.5	0.99	2258	0.7	0.1	2404	0.7	0.1
			cc	2036	1.2	0.1	0.7	0.99	0.5	2179	0.5	0.1	2343	0.6	0.1
-1	$\frac{3}{2}$	$\frac{1}{2}^-$	sc	1895	0.7	0.7	0.3	0.6	0.99	1987	0.2	0.1	2158	0.3	0.1
			cc	1884	0.7	0.7	0.0	0.5	0.99	1974	0.3	0.1	2145	0.4	0.1

TABLE III. *(Continued).*

Y	I	J^P		QDCSM						Chiral quark model			Naive quark model		
				E	S	T	ϵ_1	ϵ_2	ϵ_3	E	S	T	E	S	T
-1	$\frac{1}{2}$	$\frac{5}{2}^+$	sc	2211	1.2	0.6	0.5	0.8	0.8	2405	0.6	0.1	2539	0.7	0.1
			cc	2175	1.5	0.1	0.6	0.99	0.3	2367	0.6	0.1	2510	0.7	0.1
-2	1	$\frac{5}{2}^+$	sc	2272	1.4	0.4	0.8	0.99	0.5	2462	0.6	0.1	2539	0.7	0.1
			cc	2272	1.4	0.4	0.8	0.99	0.5	2461	0.6	0.1	2539	0.7	0.1
-2	0	$\frac{5}{2}^+$	sc	2244	1.5	0.1	0.6	0.99	0.3	2423	0.6	0.1	2539	0.7	0.1
			cc	2241	1.5	0.1	0.6	0.99	0.3	2416	0.6	0.1	2539	0.7	0.1
-3	$\frac{1}{2}$	$\frac{5}{2}^+$	sc	2323	1.4	0.1	0.7	0.99	0.3	2491	0.5	0.1	2568	0.6	0.1

effect can be replaced by the QDCSM mechanism for pentaquark systems as well. However, the naive quark model results are quite different. The naive quark model is quite possibly not a realistic one for multiquark systems even though it is a good model for single hadrons because it cannot reproduce the intermediate range NN attraction and the deuteron properties.

(iv) In QDCSM, the majority of the lowest energy states have the triangle pattern. The separations between the two diquarks are $S = 0.8 \sim 1.5$ fm and the separation between the antiquark and the center of the two diquarks is $T = 0.3 \sim 0.9$ fm, except for in a few positive parity states. In the chiral quark model and the naive quark model, the lowest energy states always have a linear pattern: the separations between the two diquarks are $S = 0.3 \sim 0.8$ fm and the separation between the antiquark to the diquark center is 0.1 fm. We don't have any experimental data to check which one is more realistic. Lattice QCD calculations might provide useful information.

There were discussions on the systematics of the states in anti-decuplet, 27-plet, and 35-plet [10,14–16,36]. These states are classified by flavor symmetry. Here, we only consider flavor symmetry of the four-quark system. When coupled to antiquarks, the states in $1_f, 8_f, 10_f, \overline{10}_f, 27_f, 35_f$ will be mixed, i.e., $[4] \otimes [11] \to [51] \oplus [411]$; $[31] \otimes [11] \to [42] \oplus [411] \oplus [321]$; $[22] \otimes [11] \to [33] \oplus [321]$; $[211] \otimes [11] \to [321] \oplus [222]$. So the states we discuss here are mixed ones. In the following we give the main features of these states in our calculation and compare them with the results of other models.

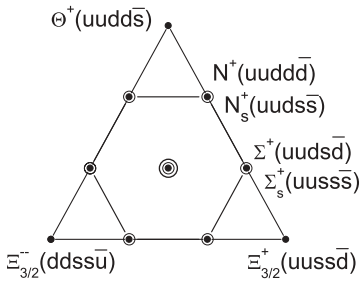

FIG. 5. Quark content of representative members of the $8_f + \overline{10}_f$ states.

(i) $8_f + \overline{10}_f$ states. The quark contents of representative states in $8_f + \overline{10}_f$ are given in Fig. 5. The mass spectrum of the states with $J^P = \frac{1}{2}^+$ in the three quark models is summarized in Fig. 6 and compared with the results of Jaffe–Wilczek [10] and the chiral soliton model [10]. The results of Bijker *et al.* [16] are also listed. Obviously, the order of the states of JW, chiral quark model, and QDCSM is similar; the chiral soliton model and the naive quark model results are different from those of the latter three. In the quark model, generally the states with more s quarks lie higher, so Σ_s with three strange quarks has the highest energy, while N without strange quarks has the lowest energy. N_s, $\Xi_{3/2}$ (with two strange quarks) and Λ, Σ, Θ^+ (with one strange quark) lie between. In the chiral soliton model Θ^+ is the lowest state, where flavor SU(3) symmetry is implied. However, the flavor SU(3) symmetry is broken by the large strange quark mass. The mass spectrum of the states with $J^P = \frac{1}{2}^-$ in the three quark models are summarized in Fig. 7 and compared with that of the chiral soliton model [36]. The results of Bijker *et al.* [16] are also listed. For $J^P = \frac{1}{2}^-$, the order of the states is different from the

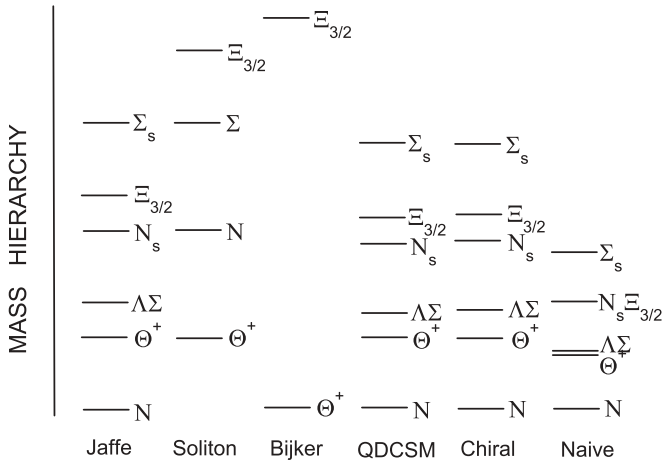

FIG. 6. Mass hierarchy in the $8_f + \overline{10}_f$ state with $J^P = \frac{1}{2}^+$ in the three quark models, compared with the mass hierarchy in Ref. [10] and Ref. [16].

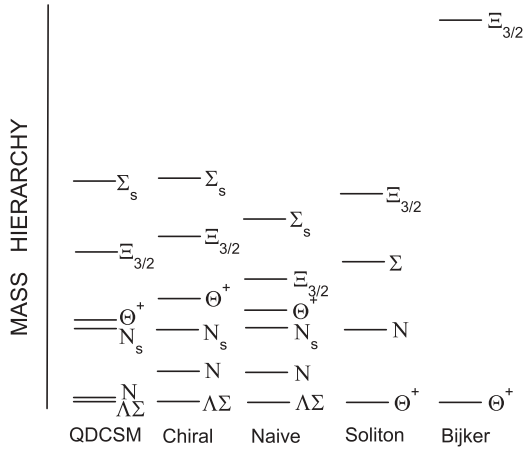

FIG. 7. Mass hierarchy in the $8_f + \overline{10}_f$ state with $J^P = \frac{1}{2}^-$ in the three quark models, compared with the mass hierarchy in Ref. [36] and Ref. [16].

order for $J^P = \frac{1}{2}^+$, but all the three quark models have similar orders. The chiral soliton model results are quite different from those of the three quark models. Other states with $J^P = \frac{3}{2}^\pm$ and $J^P = \frac{5}{2}^\pm$ are also calculated. To save space, we have not listed all the results here.

(ii) 27-plet. The quark contents of representative states in the 27-plet are given in Fig. 8. The mass spectrum of the states with $J^P = \frac{3}{2}^\pm$ in the three quark models is summarized in Figs. 9 and 10 and compared with the results of the chiral soliton model [14] and Bijker *et al*. [16]. We see again that the chiral quark model and QDCSM results are similar but quite different from the results of the chiral soliton model and the results of Bijker *et al*. [16].

(iii) 35-plet. The quark contents of representative states in the 35-plet are given in Fig. 11. The mass spectrum of the states with $J^P = \frac{5}{2}^+$ in the three quark models is summarized in Fig. 12 and compared with the results of the chiral soliton model [15] and Bijker *et al*. [16]. One sees once more that the chiral quark model and QDCSM results are similar but different from those of the chiral soliton model and Bijker *et al*. [16].

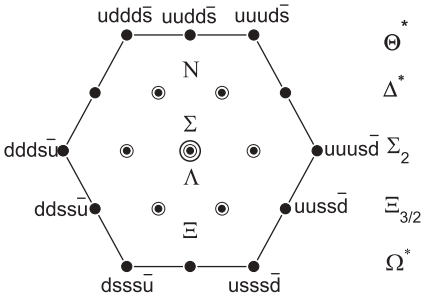

FIG. 8. Quark content of representative members of the 27-plet states.

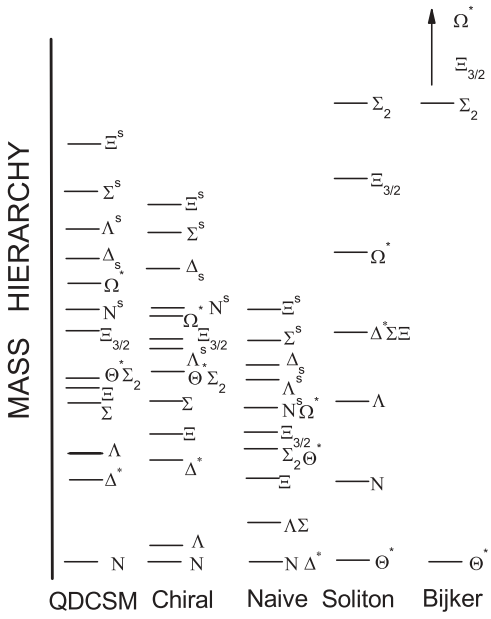

FIG. 9. Masses of states in the 27-plet with $J^P = \frac{3}{2}^-$ in the three quark models, compared with the mass in Refs. [14] and [16].

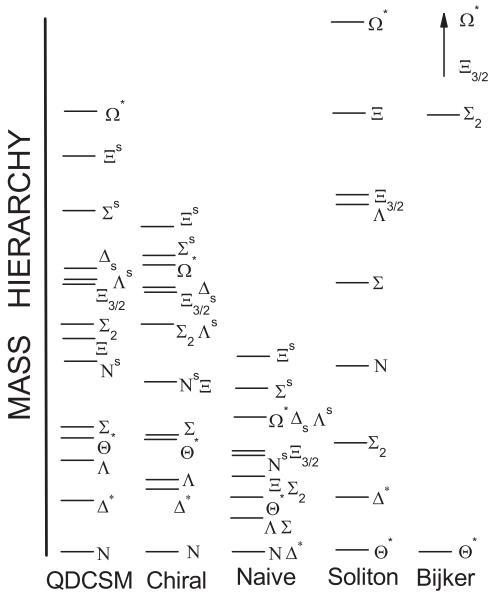

FIG. 10. Masses of states in the 27-plet with $J^P = \frac{3}{2}^+$ in the three quark models, compared with the masses in Refs. [14] and [16].

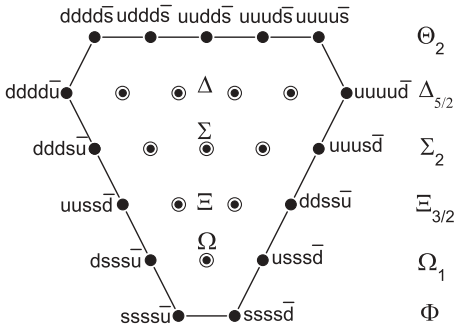

FIG. 11. Quark content of representative members of the 35-plet states.

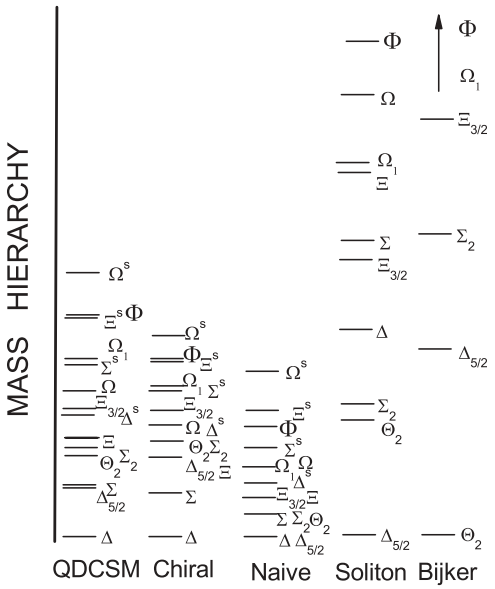

FIG. 12. Masses of states in the 35-plet with $J^P = \frac{5}{2}^+$ in the three quark models, compared with the mass in Refs. [15] and [16].

V. SUMMARY

The dibaryon states have been claimed and have disappeared a few times, the pentaquark Θ^+ might disappear, and the tetraquark states might be not confirmed. However, the multiquark state search will be continued. On the basis of QCD, multiquark components in meson and baryon cannot be denied. Meson-meson, meson-baryon, baryon-baryon, and baryon-antibaryon scattering have been measured. If one wants to understand all of these physics from quark-gluon degree of freedom one needs a few-body calculation method and the group theoretic method is one of the powerful ones. This article reports the needed group theory results for five-quark calculations within the Jaffe–Wilczek quark cluster configuration. A systematic study of all possible pentaquark states within the u, d, s three-flavor world in the three quark models is performed. The powerful feature of group theory method is shown by the large amount of spectroscopy data obtained easily with this approach.

About the physical results we emphasize, first, that in general there exists effective attraction for both parity states because of the JW hidden color configuration. Therefore, it is possible to form five-quark resonance, because once such a state is formed it cannot decay to colorful subsystems immediately and must transit to colorless subsystems through color rearrangement first and then decay. This is similar to compound nucleus formation but due to color confinement. It is a new kind microscopic resonance; we call it color confinement resonance. The transition rate is determined by the transition interaction between hidden color states to colorless ones. Up until now we did not have any idea about this transition interaction. Therefore, we cannot make any definite predictions about the width of these resonances. It is likely that lattice QCD will be able to study this transition interaction.

Second, the chiral quark model and QDCSM give similar pentaquark mass spectroscopy, which is different from that of the chiral soliton model. The SU(3) flavor symmetry is broken by the large strange quark mass. The similarity of the pentaquark mass spectroscopy of the chiral quark model and and that of QDCSM means the σ meson effect can be replaced by quark delocalization and the color screening mechanism as has been verified in *NN* intermediate range attraction.

ACKNOWLEDGMENTS

This work was supported by NSFC Grants 90503011, 10375030, and 10775072.

[1] R. L. Jaffe, Phys. Rev. Lett. **38**, 195 (1977).
[2] R. Bilger, H. A. Clement, and M. G. Schepkin, Phys. Rev. Lett. **71**, 42 (1993).
[3] T. Goldman, K. Maltman, G. J. Stephenson, K. E. Schmidt, and F. Wang, Phys. Rev. C **39**, 1889 (1989); J. L. Ping, F. Wang, and T. Goldman, Nucl. Phys. **A688**, 871 (2001); J. L. Ping, H. R. Pang, F. Wang, and T. Goldman, Phys. Rev. C **65**, 044003 (2002).
[4] T. Goldman, K. Maltman, G. J. Stephenson, K. E. Schmidt, and F. Wang, Phys. Rev. Lett. **59**, 627 (1987); H. R. Pang, J. L. Ping, F. Wang, T. Goldman, and E. Zhao, Phys. Rev. C **69**, 065207 (2004); H. R. Pang, J. L. Ping, C. L. Chen, F. Wang, and T. Goldman, *ibid.* **70**, 035201 (2004).
[5] V. B. Kopeliovich, B. Schwesinger, and B. E. Stern, Phys. Lett. **B242**, 145 (1990); Q. B. Li, P. N. Shen, Z. Y. Zhang, and Y. W. Yu, Nucl. Phys. **A683**, 487 (2001); H. R. Pang, J. L. Ping, F. Wang, and T. Goldman, Phys. Rev. C **66**, 025201 (2002).
[6] T. Nakano, D. S. Ahn, J. K. Ahn *et al.*, Phys. Rev. Lett. **91**, 012002 (2003).
[7] K. Hicks, Prog. Part. Nucl. Phys. **55**, 647 (2005), and references therein; V. D. Burkert, Int. J. Mod. Phys. A **21**, 1764 (2006).
[8] M. Oka, Prog. Theor. Phys. **112**, 1 (2004); K. Goeke *et al.*, Prog. Part. Nucl. Phys. **55**, 350 (2005), and references therein; S. L. Zhu, Int. J. Mod. Phys. A **20**, 1548 (2005), and references therein.
[9] J. L. Ping, D. Qing, F. Wang, and T. Goldman, Phys. Lett. **B602**, 197 (2004).
[10] R. Jaffe and F. Wilczek, Phys. Rev. Lett. **91**, 232003 (2003).
[11] M. Karliner and H. J. Lipkin, Phys. Lett. **B575**, 249 (2003).
[12] X. C. Song and S. L. Zhu, Mod. Phys. Lett. A **19**, 2791 (2004).
[13] CLAS Collaboration, Phys. Rev. Lett. **97**, 032001 (2006); **96**, 042001 (2006); **96**, 212001 (2006); **97**, 102001 (2006); Phys. Rev. D **74**, 032001 (2006); J. M. Link *et al.* (FOCUS Collaboration), Phys. Lett. **B639**, 604 (2006); M. Abdel-Bary *et al.* (COSY-TOF Collaboration), Phys. Lett. **B649**, 252 (2007).
[14] B. Wu and B. Q. Ma, Phys. Rev. D **69**, 077501 (2004); Q. H. Zhou and B. Q. Ma, Eur. Phys. J. C **49**, 897 (2007).
[15] B. Wu and B. Q. Ma, Phys. Rev. D **70**, 094042 (2004).
[16] R. Bijker *et al.*, Eur. Phys. J. A **22**, 319 (2004).
[17] D. Qing, X. S. Chen, and F. Wang, Phys. Rev. C **57**, R31 (1998); Phys. Rev. D **58**, 114032 (1998).
[18] B. S. Zou and D. O. Riska, Phys. Rev. Lett. **95**, 072001 (2005).

[19] B. Aubert *et al*., Phys. Rev. Lett. **90**, 242001 (2003); S. K. Choi *et al*., Phys. Rev. Lett. **91**, 262001 (2003); A. V. Evdokimov *et al*. (SELEX Collaboration), Phys. Rev. Lett. **93**, 242001 (2004); B. Aubert *et al*., Phys. Rev. Lett. **95**, 142001 (2005); R. L. Jaffe, Phys. Rep. **409**, 1 (2005).

[20] F. Okiharu, H. Suganuma, and T. T. Takahashi, Phys. Rev. D **72**, 014505 (2005).

[21] M. W. Paris and V. R. Pandharipande, Phys. Rev. C **62**, 015201 (2000).

[22] E. Santopinto and G. Galata, Phys. Rev. C **75**, 045206 (2007).

[23] F. Wang, J. L. Ping, and T. Goldman, Phys. Rev. C **51**, 1648 (1995).

[24] F. Wang, J. L. Ping, G. H. Wu, L. J. Teng, and T. Goldman, Phys. Rev. C **51**, 3411 (1995).

[25] T. Goldman *et al*., Mod. Phys. Lett. A **13**, 59 (1998); H. R. Pang, J. L. Ping, F. Wang, and T. Goldman, Phys. Rev. C **65**, 014003 (2001).

[26] A. De Rujula, H. Georgi, and S. L. Glashow, Phys. Rev. D **12**, 147 (1975); N. Isgur and G. Karl, *ibid.* **18**, 4187 (1978); **19**, 2653 (1979); **20**, 1191 (1979).

[27] A. Valcarce, H. Garcilazo, F. Fernandez, and P. Gonzalez, Rep. Prog. Phys. **68**, 965 (2005).

[28] F. Wang, G. H. Wu, L. J. Teng, and T. Goldman, Phys. Rev. Lett. **69**, 2901 (1992).

[29] J. Q. Chen, J. L. Ping, and F. Wang, *Group Representation Theory for Physicists* (World Scientific, Singapore, 2002).

[30] J. Q. Chen, X. B. Wu, and M. J. Gao, *Tables of the SU(mn)⊃SU(m)×SU(n) Coefficients of Fractional Parentage* (World Scientific, Singapore, 1991).

[31] M. Harvey, Nucl. Phys. **A352**, 301 (1981); **481**, 834 (1988).

[32] J. Q. Chen, Y. J. Shi, D. H. Feng, and M. Vallieres, Nucl. Phys. **A393**, 122 (1983).

[33] G. H. Wu, J. L. Ping, L. J. Teng, F. Wang, and T. Goldman, Nucl. Phys. **A673**, 279 (2000); J. L. Ping, F. Wang, and T. Goldman, Nucl. Phys. **A657**, 95 (1999).

[34] H. X. Huang, C. R. Deng, J. L. Ping, F. Wang, and T. Goldman, arXiv:0711.1649.

[35] L. Z. Chen, H. R. Pang, H. X. Huang, J. L. Ping, and F. Wang, Phys. Rev. C **76**, 014001 (2007).

[36] B. Wu and B. Q. Ma, Phys. Rev. D **70**, 097503 (2004).